Parametrization of electron spin resonance spectra of even and odd isotopes of Mo^{5+} in tungsten phosphate glasses

1991 J. Phys.: Condens. Matter 3 6209

(http://iopscience.iop.org/0953-8984/3/33/001)

J. Phys.: Condens. Matter 3 (1991) 6209–6223. Printed in the UK

Parametrization of electron spin resonance spectra of even and odd isotopes of Mo^{5+} in tungsten phosphate glasses

Alla Bals† and Jānis Kliava‡

† Institute of Solid State Physics, 8 Ķengaraga ielā, 226063 Rīgā, Latvia, USSR

‡ Faculty of Physics and Mathematics, University of Latvia, 19 Raiņa bulvārī, 226098 Rīgā, Latvia, USSR

Received 14 December 1990, in final form 14 March 1991.

Abstract. By computer simulation of the electron spin resonance spectra of even and odd isotopes of Mo^{5+} in WO_3–BaO–P_2O_5 glasses of various compositions, the characteristics of the distributions of g values and hyperfine structure parameters have been deduced. Using these data, the characteristics of the distributions of energy level splittings and bonding parameters of Mo^{5+} are separately determined. Variations of these parameters in relation to the glass composition are discussed. The magnitudes of the relative distribution widths, approximately 10% for the energy level splittings and a few per cent for the bonding parameters, reflect the degree of short-range disorder in the environment of Mo^{5+} ions.

1. Introduction

According to the random network model (Zachariasen 1932) the structure of glass consists of well ordered corner-sharing coordination polyhedra of network-forming ions; network modifiers occupy voids of the resulting structure and therefore, presumably, possess no distinct type of environment. However, recent extended x-ray absorption fine structure (EXAFS) (Greaves 1985, Studer *et al* 1986) and electron spin resonance (ESR) (Kliava 1986, 1988) data suggest a high degree of ordering in the surroundings of network modifiers as well. Thus, important amendments to the traditional concept of glass structure are required; a more adequate picture appears to be a network made of at least two types of well ordered coordination polyhedra: those of network formers and network modifiers, which share common corners.

In the present study, ternary phosphate glasses of the tungsten trioxide–barium oxide–phosphorus pentoxide system (WO_3–BaO–P_2O_5) have been investigated using the structure-sensitive ESR method.

In phosphate glasses, the structural role of phosphorus as the network former and that of an alkaline-earth ion, e.g. barium, as the network modifier is well established (Rawson 1967). However, the presence in the glass of the third component, tungsten trioxide, greatly complicates the problem of understanding the structure of ternary phosphate glass. Therefore, it seems interesting to investigate the correlation between the composition and structural properties in such glasses. Earlier studies by Bielis and Millere (1977) on this system, as well as on the related one, WO_3–CaO–P_2O_5 (Bielis and

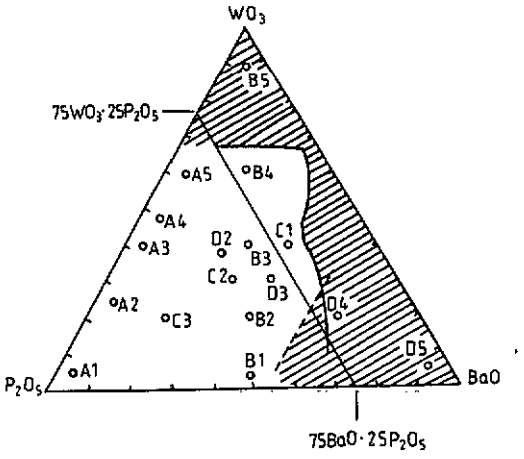

Figure 1. Compositions (mol%) of glass samples indicated on the ternary phase diagram of the WO_3–BaO–P_2O_5 system. Areas *outside* the glass-forming region, bounded by the irregular and dashed lines, are shaded. The orthophosphate line connects the $75WO_3 \cdot 25P_2O_5$ and $75BaO \cdot 25P_2O_5$ points.

Millere 1975), indicate that the glass-forming region in the tungsten trioxide–alkaline-earth oxide–phosphorus pentoxide system (see figure 1) consists of two subregions. The boundary between these subregions coincides with the orthophosphate line corresponding to the molar compositions $(75 - x)WO_3 \cdot xBaO \cdot 25P_2O_5$ $(0 \leqslant x \leqslant 75)$. With glasses containing more than 25% of phosphorus pentoxide no detectable crystallization occurs, whereas glasses with smaller P_2O_5 content possess a high crystallization ability. The existence of these two subregions is indicative of different structural roles of tungsten. Bielis and Millere (1975, 1977) tentatively assumed that below the orthophosphate line tungsten acts as a network modifier, whereas above this line it may take the role of network former.

2. Samples and experimental results

Ternary phosphate glasses of the tungsten trioxide–barium oxide–phosphorus pentoxide system of different molar compositions have been chosen for this study.

The relation of these compositions to the glass-forming region in this system is shown in figure 1.

With no special doping of the WO_3–BaO–P_2O_5 system only the ESR spectrum of W^{5+} is observed in glasses of some compositions. However, its intensity depends to a great extent on the method of preparing the glass samples. Another difficulty related to the ESR of W^{5+} in glass is the relative smallness of the nuclear magnetic momentum of tungsten; as a result, the hyperfine structure (HFS) in X-band ESR spectra of W^{5+} in glasses is not resolved.

To overcome all these difficulties, we have carried out this study using molybdenum-doped glasses. It is expected that Mo^{5+} and W^{5+} occupy one and the same type of site in the glass structure (Bals and Kliava 1983). (Mo^{5+} ion substitutes for its analogue W^{5+}.) In our previous studies (Bals *et al* 1980, Bals and Kliava 1983, Kliava and Bals 1984) glasses doped with molybdenum trioxide containing Mo with natural isotopic abundance (74.62% of even isotopes with nuclear spin $I = 0$ and 25.38% of odd isotopes with $I = 5/2$) were used. In the present work, isotopically enriched dopants have been used: each

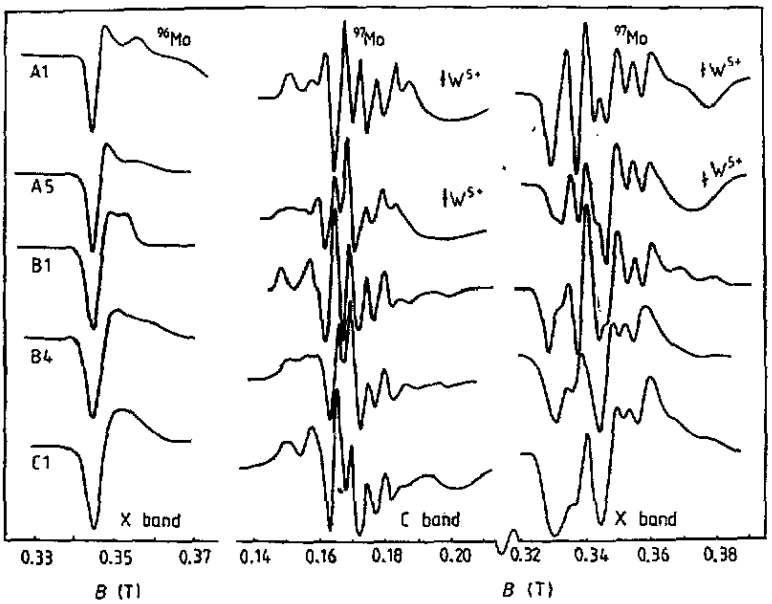

Figure 2. Representative room-temperature X- and C-band ESR spectra of WO_3–BaO–P_2O_5 glasses doped with isotopically enriched molybdenum trioxide (see text). The sample compositions are given in table 1.

Table 1. Molar compositions of the glass samples.

	A1	A5	B1	B4	C1
WO_3	5	60	3	60	40
BaO	5	5	48.5	20	40
P_2O_5	90	35	48.5	20	20

series of glasses has been doped with MoO_3 enriched with either 98.6% of ^{96}Mo or 92.7% of ^{97}Mo.

The method of preparing the glass samples was as follows. As starting materials, reagent-grade barium carbonate, 85% orthophosphorous acid and extra-pure tungsten trioxide were used. The dopants were added to batches in the form of molybdenum trioxide (0.05 mol% over 100 mol%). Such a small amount of dopant precludes dipole–dipole broadening of ESR spectral features. Mixtures were kept in air for 24 h, then fused in an electric muffle (raising the temperature to 1100 °C for 4 h and keeping at maximum temperature for 1 h). The melts were quenched by pouring onto a massive metallic plate.

The ESR spectra have been recorded with X-band, 9323 MHz, and C-band, 4476 MHz, spectrometers at temperatures between 120 and 300 K. No appreciable variation in the spectral shapes with temperature could be detected within this range.

Figure 2 exhibits a representative series of experimental ESR spectra from different parts of the glass-forming region, which have been chosen for computer simulations. Compositions of the corresponding glass samples are given in table 1. The only charge

state of molybdenum observed in the ESR has been Mo^{5+} (electron spin $S = 1/2$). Since the spectral shapes for the even isotope, $^{96}Mo^{5+}$, at X and C bands are very similar, only the X-band spectra are shown in this case.

3. Calculation of spectra

The spin Hamiltonian for Mo^{5+} ions in the case of even isotopes ($I = 0$) includes only the Zeeman interaction:

$$\mathcal{H} = \beta \boldsymbol{B}\mathbf{g}\boldsymbol{S} \tag{1}$$

where β is the Bohr magneton, $\boldsymbol{B}$ is the magnetic field and $\mathbf{g}$ is the $\mathbf{g}$ matrix. In the case of odd isotopes ($I = 5/2$), the hyperfine interaction should be added to the spin Hamiltonian:

$$\mathcal{H} = \beta \boldsymbol{B}\mathbf{g}\boldsymbol{S} + \boldsymbol{S}\mathbf{A}\boldsymbol{I} \tag{2}$$

where $\mathbf{A}$ is the HFS matrix.

In glass, the short-range disorder inherent in the vitreous state manifests itself in a distribution of the spin Hamiltonian parameters (Peterson *et al* 1974, Taylor *et al* 1975, Griscom 1980, Kliava 1986, 1988). Parametrization of the corresponding ESR spectra has become feasible only with the advent of computer simulation techniques.

The general expression of ESR spectra in glass can be written as follows (Kliava 1986, 1988):

$$\mathcal{P}(B) = \frac{1}{4\pi}\int_{\Omega}\int_{H} P(\boldsymbol{H})W(\boldsymbol{H}, \boldsymbol{\Omega})\left|\mathrm{d}B_r(\boldsymbol{H}, \boldsymbol{\Omega})/\mathrm{d}\nu_c\right| F[B - B_r(\boldsymbol{H}, \boldsymbol{\Omega}), \Delta B]\,\mathrm{d}V(\boldsymbol{H}, \boldsymbol{\Omega}) \tag{3}$$

where $P(\boldsymbol{H})$ is the joint probability density of the spin Hamiltonian parameters $\boldsymbol{H} = (H_1, H_2, \ldots, H_N)$, $W(\boldsymbol{H}, \boldsymbol{\Omega})$ is the transition probability, $\boldsymbol{\Omega} = (\vartheta, \varphi)$, ϑ and φ being, respectively, the polar and azimuthal angles of the vector $\boldsymbol{B}$ in the principal coordinate system of the spin Hamiltonian, B_r is the resonance magnetic field, ν_c is the microwave frequency (which is kept constant in a field-swept ESR experiment) and F is the lineshape with linewidth ΔB determined by spin–lattice and spin–spin interactions. The integration in (3) is performed over all orientations of $\boldsymbol{B}$, i.e. $0 \leqslant \vartheta < \pi$, $0 \leqslant \varphi < 2\pi$, and over distributed values of $H_1, \ldots, H_N$.

In our simulations, F has been chosen in the form of a Lorentzian, while $P(\boldsymbol{H})$ had the form of a multidimensional Gaussian. Referring to the spin Hamiltonian (1), $P(\boldsymbol{g})$, the joint probability density of $\boldsymbol{g}$ values, depends on as many as nine parameters, which are to be deduced from the computer simulations: three mean values, $\bar{g}_x, \bar{g}_y, \bar{g}_z$, three root-mean-square (RMS) deviations, $\Delta g_x, \Delta g_y, \Delta g_z$, and three correlation coefficients, $\rho(g_x, g_y), \rho(g_y, g_z), \rho(g_x, g_z)$. In the case of spin Hamiltonian (2), $P(\boldsymbol{H})$ in Gaussian form depends on six mean values, $\bar{g}_i, \bar{A}_i$, six RMS deviations, $\Delta g_i, \Delta A_i$, and 15 correlation coefficients of the type $\rho(g_i, g_j)$, $\rho(A_i, A_j)$, $\rho(g_i, A_j)$, where $i, j = x, y, z$. Furthermore, for low-symmetry centres, the principal axes of $\mathbf{g}^2$ and $\mathbf{A}^2$ tensors do not necessarily coincide. We are referring to $\mathbf{g}^2$ and $\mathbf{A}^2$ tensors, since $\mathbf{g}$ and $\mathbf{A}$ in the case of lower-than-rhombic symmetry are *not* true tensors (see e.g. Pilbrow and Lowrey 1980). In this case, the three Eulerian angles describing the mutual orientation of principal axes of $\mathbf{g}^2$ and $\mathbf{A}^2$ tensors should be taken into account as additional spin Hamiltonian parameters. This

bring about in $P(\boldsymbol{H})$ three additional mean values and RMS deviations, as well as a great number of correlation coefficients. It is evident that the number of parameters that are to be extracted from an ESR spectrum is too high and a unique (unambiguous) set of best-fit parameters can hardly be determined from computer simulations.

In order to simplify this problem to some extent, we confine the description of the mutual orientation of the principal axes of $\mathbf{g}^2$ and $\mathbf{A}^2$ tensors to a single angle ψ, the one between the z axes. (Furthermore, we neglect an eventual distribution of this angle.) Then in the principal axes system of $\mathbf{g}^2$ tensor the HFS matrix is as follows:

$$\mathbf{A} = \begin{pmatrix} A_x \cos^2\psi + A_z \sin^2\psi & 0 & (A_x - A_z)\sin\psi\cos\psi \\ 0 & A_y & 0 \\ (A_x - A_z)\sin\psi\cos\psi & 0 & A_x \sin^2\psi + A_z\cos^2\psi \end{pmatrix}. \tag{4}$$

Strictly speaking, this approximation provides satisfactory results only for nearly axial symmetry of the surroundings of Mo^{5+} ions and hence of the spin Hamiltonian parameters: $\bar{g}_x \simeq \bar{g}_y, \bar{A}_x \simeq \bar{A}_y$. Fortunately, the results of our computer simulations (see table 2 below) clearly demonstrate that the difference between $\bar{g}_x$ and $\bar{g}_y$ is much less than the difference between any of these values and $\bar{g}_z$; analogous relations hold between $\bar{A}_x, \bar{A}_y$ and $\bar{A}_z$. Moreover, near-to-axial symmetry is confirmed with the bulk of existing ESR data on Mo^{5+} in glasses (e.g. Griscom 1980, Kliava 1986, 1988).

The resonance magnetic field to second order in perturbation theory was calculated by Golding and Tennant (1973) and Daul *et al* (1981). In the actual case here, the corresponding expression reduces to the following form:

$$B_r = \frac{h\nu_c}{g\beta} - Km_I - \frac{g\beta}{2h\nu_c}\{(L^2 - K^2)m_I^2 + \tfrac{1}{2}[\mathrm{Tr}(\mathbf{A}^2) - L^2][I(I+1) - m_I^2]\} \tag{5}$$

where m_I is the magnetic quantum number for the nuclear spin,

$$\begin{aligned} K^2 = {} & [G_x^2(A_{xx}^2 + A_{xz}^2) + G_y^2 A_{yy}^2 + G_z^2(A_{zz}^2 + A_{xz}^2) \\ & + 2G_xG_zA_{xz}(A_{xx} + A_{zz})]/(G_x^2 + G_y^2 + G_z^2) \end{aligned} \tag{6}$$

$$\begin{aligned} L^2 = {} & \{G_x^2[(A_{xx}^2 + A_{xz}^2)^2 + A_{xz}^2(A_{xx} + A_{zz})^2] + G_y^2 A_{yy}^4 \\ & + G_z^2[A_{xz}^2(A_{xx} + A_{zz})^2 + (A_{zz}^2 + A_{xz}^2)^2] \\ & + 2G_xG_zA_{xz}(A_{xx} + A_{zz})(A_{xx}^2 + A_{zz}^2 + 2A_{xz}^2)\}/[G_x^2(A_{xx}^2 + A_{xz}^2) \\ & + G_y^2A_{yy}^2 + G_z^2(A_{zz}^2 + A_{xz}^2) + 2G_xG_zA_{xz}(A_{xx} + A_{zz})] \end{aligned} \tag{7}$$

and

$$\mathrm{Tr}(\mathbf{A}^2) = A_{xx}^2 + A_{yy}^2 + A_{zz}^2 + 2A_{xz}^2. \tag{8}$$

Here $G_i = g_i l_i, i = x, y, z, l_x = \sin\vartheta\cos\varphi, l_y = \sin\vartheta\sin\varphi, l_z = \cos\vartheta$ and A_{ij} are elements of the HFS matrix.

In spite of the assumptions made above, the number of simulation parameters in the case of the spin Hamiltonian (2) still remains too high. Therefore, for the natural isotopic abundance of molybdenum, no reliable estimation of HFS parameters is feasible. Yet, with isotopically enriched molybdenum, a *gradual* (two-step) parametrization can be carried through. At the first step, by computer simulating the ESR spectrum of the even isotope, $^{96}Mo^{5+}$, the $\bar{g}_i$, Δg_i and $\rho(g_i, g_j)$ parameters are determined. At the second step,

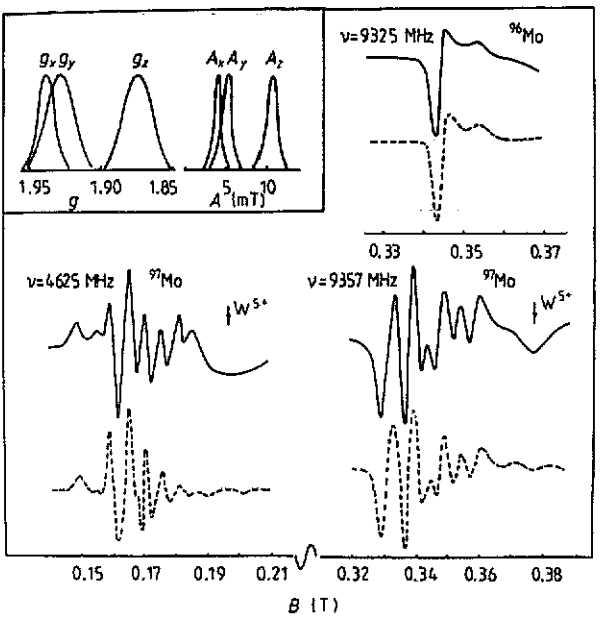

Figure 3. Results of computer simulations of the $^{96}Mo^{5+}$ (X band) and $^{97}Mo^{5+}$ (X and C bands) ESR spectra in A1 glass. Full curves: the experimental spectra. Broken curves: the computer-generated best-fit spectra. The simulation parameters are given in table 2. Inset: distributions of g values and HFS parameters scaled in proportion to their relative contributions to the resonance magnetic fields.

the remaining parameters are deduced from computer simulations of the ESR spectrum of the odd isotope, $^{97}Mo^{5+}$, in glass of the same composition.

The accuracy of parametrization can be further enhanced by carrying out the simulation of spectra recorded at two different microwave frequencies. One can see from figure 2 that the spectral shapes for $^{97}Mo^{5+}$ are totally different at X and C bands, while the spin Hamiltonian parameters involved should evidently be the same.

Figures 3 and 4 illustrate the results of computer fitting to the experimental ESR spectra. The best-fit parameters obtained are summarized in table 2.

4. Discussion

4.1. Symmetry of 'average' paramagnetic sites

We begin our analysis with mean spin Hamiltonian parameters, a full set of which describes an 'average' paramagnetic site, i.e. one characterized by structural parameters obtained by statistically averaging over the whole ensemble of Mo^{5+} sites in a glass sample.

From the general aspect of ESR spectral shapes (see figure 2), as well as from the best-fit parameters summarized in table 2, mainly from the HFS matrix elements, the existence of two somewhat different Mo^{5+} sites can be inferred. The first site is observed *below* the orthophosphate line, i.e. in A1, A5 and B1 glasses, while the second site predominates *above* the orthophosphate line, in B4 and C1 glasses.

A comparison of the $\bar{g}_i$ values, as determined from the computer simulations, with g values characteristic of Mo^{5+} ions having different coordination numbers, $C = 4, 5, 6$ (Latef *et al* 1987, Louis and Che 1987), leads one to opt for C between 5 and 6. This value is consistent with a molybdenyl complex, in which case one molybdenum–oxygen

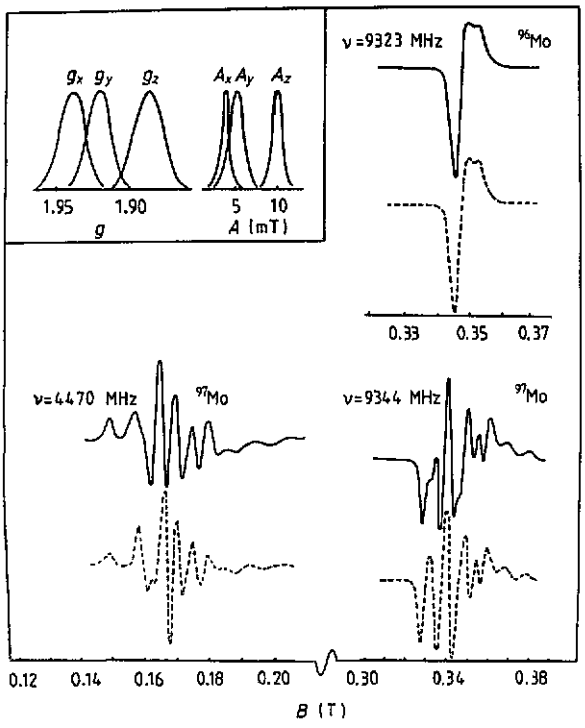

Figure 4. Results of computer simulations of the $^{96}Mo^{5+}$ (X band) and $^{97}Mo^{5+}$ (X and C bands) ESR spectra in B1 glass. See the legend of figure 3 for further details.

Table 2. Best-fit parameters of the joint probability density $P(g, A)$ for Mo^{5+} in WO_3–BaO–P_2O_5 glasses (the HFS parameters are given in 10^{-4} T)[a].

	A1	A5	B1	B4	C1
$\bar{g}_x$	1.937(2)	1.935(2)	1.939(2)	1.934(2)	1.934(2)
$\bar{g}_y$	1.928(2)	1.924(2)	1.920(2)	1.913(2)	1.913(2)
$\bar{g}_z$	1.874(2)	1.865(3)	1.887(2)	1.849(2)	1.865(2)
Δg_x	0.0067(3)	0.0070(3)	0.0082(3)	0.0098(3)	0.0110(3)
Δg_y	0.0095(3)	0.0095(3)	0.0078(3)	0.0141(2)	0.0140(3)
Δg_z	0.0097(3)	0.0179(3)	0.0093(3)	0.0215(3)	0.0185(3)
$\bar{A}_x$	54(2)	48(2)	53(2)	49(2)	53(2)
$\bar{A}_y$	42(3)	42(3)	39(3)	35(3)	30(3)
$\bar{A}_z$	104(1)	104(1)	100(1)	93(1)	87(1)
ΔA_x	6(2)	7(2)	6(2)	5(2)	8(2)
ΔA_y	4(2)	6(2)	4(2)	5(2)	8(2)
ΔA_z	6(1)	8.5(10)	6(1)	7(1)	9.5(10)

[a] Figures in parentheses are the standard errors in the last digit. The correlation coefficients between different spin Hamiltonian parameters lie within the limits −0.5 to +0.5. $\psi = 0(5)°$.

bond is substantially shortened, while oxygen occupying the *trans* position to the first one is located at a much longer distance than the remaining ones (or is even altogether absent) (Griscom 1980, Studer *et al* 1988). Consequently, a tungstyl-type surrounding

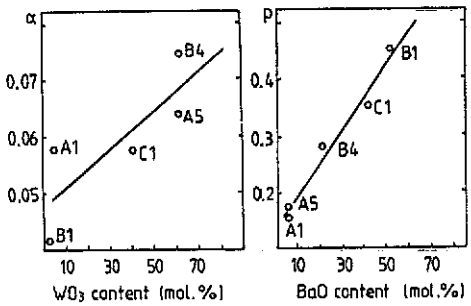

Figure 5. Degrees of axial and rhombic distortions as functions of glass composition. α and ρ are defined in equations (9). The straight lines are guides to the eye.

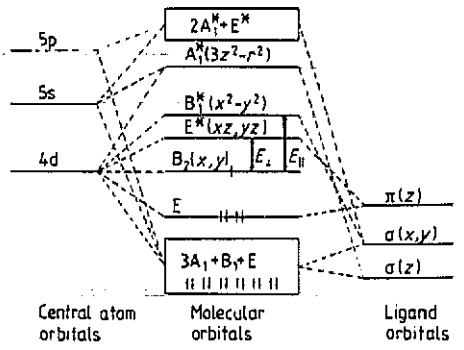

Figure 6. Energy level scheme for a molybdenyl complex of C_{4v} symmetry. Asterisks mark antibonding orbitals. π-bonding with equatorial ligands is neglected for simplicity. The unpaired electron occupies the B_2 orbital.

can be inferred for W^{5+} ions in these glasses. Note that the above-mentioned data on crystallization of ternary phosphate glasses also provide evidence in support of sixfold coordination of tungsten.

Variations of the g values for Mo^{5+} ions with glass composition (see table 2) can be characterized by the degree of axial distortion, α, and the degree of rhombic distortion, ρ, determined as follows:

$$\alpha = \tfrac{1}{2}(\bar{g}_x + \bar{g}_y) - \bar{g}_z \qquad \rho = (\bar{g}_x - \bar{g}_y)/\alpha. \tag{9}$$

Analogous parameters can be defined for the **A** matrix elements; however, these would be of less use, since anisotropy of the **g** matrix is directly related to symmetry of a paramagnetic centre, whereas anisotropy of the **A** matrix to a first approximation is due to dipole–dipole interactions. Parameters α and ρ are shown in figure 5.

The A1 glass network for the most part is formed by phosphorus–oxygen tetrahedra. Because of their low concentration, tungsten ions here are supposed to act as network modifiers, building themselves among PO_4 structural units. In this glass the most probable next nearest neighbours (atoms of the second coordination shell) of tungsten, and presumably of molybdenum, are phosphorus atoms. In A5 glass the most probable next nearest neighbours of tungsten (and molybdenum) are both phosphorus and tungsten. In B1 glass the likely pretenders to this role are phosphorus and barium. In B4 and C1 glasses all three ions, phosphorus, tungsten and barium, are supposed to occupy the second shell of Mo^{5+} with comparable probabilities (if one assumes a purely statistical (random) distribution of these ions in the glass structure).

The above considerations can to a certain extent account for the observed variations in the degree of distortion of the Mo^{5+} surroundings with glass composition (see figure 5). Indeed, the lowest degree of rhombic distortion is observed in A1 glass, the intermediate ones in A5, B4 and C1 glasses and the highest one in B1 glass. A comparison of the ionic radii of eventual next nearest neighbours of Mo^{5+} ions, i.e. P^{5+} (0.31 Å), W^{5+} (0.76 Å) and Ba^{2+} (1.49 Å) (Shannon and Prewitt 1969), indicates that rhombic distortion of coordination polyhedra of molybdenum is due to the difference in size of ions forming the second coordination shell of the paramagnetic ion.

The dependence on glass composition of the parameter α exhibits a more complex behaviour. Attention is drawn, first of all, to the fact that α has the lowest value in B1 glass, intermediate ones in A1 and C1 glasses and the highest values in A5 and B4 glasses (see figure 5). Thus, it can be concluded that one of the main causes of axial distortion in the environment of molybdenum and, presumably, of tungsten is a high tungsten oxide content.

4.2. Estimation of the mean bonding parameters

In order to gain further insight into the observed variations of the spin Hamiltonian parameters with glass composition, we can calculate the concomitant variations in the bonding parameters, using the molecular orbital approach. Since the symmetry of 'average' paramagnetic sites of Mo^{5+} in ternary phosphate glasses turns out to be nearly axial (see table 2), one can denote

$$\begin{aligned} \bar{g}_\perp &= \tfrac{1}{2}(\bar{g}_x + \bar{g}_y) \qquad & \bar{g}_\parallel &= \bar{g}_z \\ \bar{A}_\perp &= \tfrac{1}{2}(\bar{A}_x + \bar{A}_y) \qquad & \bar{A}_\parallel &= \bar{A}_z \end{aligned} \tag{10}$$

and further consider axially symmetric ions having d^1 electronic configuration, C_{4v} symmetry and hence d_{xy} ground state. In this case the molecular orbitals involved (De Armond *et al* 1965, Hecht and Johnston 1967) are (see figure 6):

$$\begin{aligned} |B_2\rangle &= \beta_2|d_{xy}\rangle + \beta_2'|b_2\rangle \\ |E\rangle &= \begin{cases} \varepsilon|d_{xz}\rangle + \varepsilon'|e_x\rangle \\ \varepsilon|d_{yz}\rangle + \varepsilon'|e_y\rangle \end{cases} \\ |B_1\rangle &= \beta_1|d_{x^2-y^2}\rangle + \beta_1'|b_1\rangle \end{aligned} \tag{11}$$

where the non-primed and primed coefficients determine, respectively, the contributions of the Mo^{5+} orbitals and of ligand orbitals (group orbitals of appropriate symmetry).

Approximate expressions describing the relationship between the spin Hamiltonian parameters and the covalent bonding parameters can be written as follows (De Armond *et al* 1965, Hecht and Johnson 1967):

$$g_\parallel = g_e(1 - 4\lambda\beta_1^2\beta_2^2/E_\parallel) \tag{12}$$

$$g_\perp = g_e(1 - \lambda\beta_1^2\varepsilon^2/E_\perp) \tag{13}$$

$$A_\parallel = P[-\beta_2^2(\kappa + \tfrac{4}{7}) + g_\parallel - g_e + \tfrac{3}{7}(g_\perp - g_e)] \tag{14}$$

$$A_\perp = P[-\beta_2^2(\kappa - \tfrac{2}{7}) + \tfrac{11}{14}(g_\perp - g_e)] \tag{15}$$

where $g_e = 2.0023$, λ is the spin–orbit coupling constant, β_1, β_2 and ε describe, respectively, the covalency of σ and π bonding with equatorial ligands and π bonding with polar ligands, $E_\parallel = E(B_1^*) - E(B_2)$ and $E_\perp = E(E^*) - E(B_2)$ are splittings between the corresponding energy levels, P is the dipolar term and κ is the Fermi contact term, which accounts for the isotropic HF interaction.

To estimate the mean bonding parameters, the following values have been used (in cm^{-1}): $P = -55 \times 10^{-4}$, $\lambda = 820$ (Che *et al* 1979). In connection with the choice of $\bar{E}_\parallel$ and $\bar{E}_\perp$ a few remarks should be made. Since in tungsten phosphate glasses the molybdenum oxide content is low, these parameters cannot be directly determined. Indeed, as one

Table 3. Characteristics of distributions (mean values and root-mean-square deviations) of the energy level splittings (in cm^{-1}) and bonding parameters for Mo^{5+} in WO_3–BaO–P_2O_5 glasses obtained from computer simulations of the ESR spectra[a].

	A1	A5	B1	B4	C1
$\overline{\beta_2^2}$	0.993	0.999	0.978	0.936	0.870
$\overline{\beta_1^2}$	0.433	0.461	0.396	0.549	0.530
$\overline{\varepsilon^2}$	0.643	0.667	0.681	0.769	0.828
$\bar{\kappa}$	1.164	1.128	1.138	1.036	1.051
$\Delta E_\parallel$	1090	2320	1220	2320	1880
	1660	2870	1770	3080	2960
$\Delta E_\perp$	1520	1240	1400	1800	1800
	1740	1690	1650	2270	2380
$\Delta\beta_2^2$	0.140	0.054	0.040	0.061	0.064
	0.0133	0.0144	0.0137	0.022	0.0154
$\Delta\kappa$	0.084	0.099	0.086	0.083	0.157
	0.073	0.091	0.075	0.069	0.142

[a] For all samples $\bar{E}_\parallel \approx 23000$, $\bar{E}_\perp = 15000$ have been assumed. The values of $\Delta E_\parallel$, $\Delta E_\perp$, $\Delta\beta_2^2$ and $\Delta\kappa$ above and below the horizontal bars correspond, respectively, to $\rho(h_i, h_j) = 0$ for $i \neq j$ and to $\rho(h_i, h_j)$ chosen in accordance with (22). Values of $\Delta\beta_2^2$ and $\Delta\varepsilon^2$ can be estimated using equations (21).

can see from the optical absorption spectra obtained by Selvaraj and Rao (1988), for Mo^{5+} and W^{5+} the optical bands due to the d–d transitions, in contrast to the ESR bands, overlap almost completely. Selvaraj and Rao (1988) and Studer *et al* (1988) believe that the split absorption band of Mo^{5+} and W^{5+} in the range between approximately 11000 and 18000 cm^{-1} comprises both $B_2 \rightarrow E^*$ and $B_2 \rightarrow B_1^*$ transitions (see figure 6). However, these authors do not take into account the fact that, as our ESR data have demonstrated (see Bals *et al* 1980, Bals and Kliava 1983, Kliava and Bals 1984, table 2 in present paper), the actual symmetry of Mo^{5+} (and W^{5+}) is lower than axial. Therefore, our belief is that the above-mentioned absorption bands correspond to $B_2 \rightarrow E^*$ transition split by the rhombic component of the ligand field. If this is the case, the $B_2 \rightarrow B_1^*$ absorption band should occur at much higher energies, presumably, around 25000 cm^{-1} (Goldstein *et al* 1987). Unfortunately, in the same range ligand-to-metal charge transfer bands can be observed (see e.g. Selvaraj and Rao 1988).

So, for $\bar{E}_\parallel$ and $\bar{E}_\perp$ we have chosen the following values (in cm^{-1}): $E_\parallel = 23000$, $E_\perp = 15000$. These values can be considered as typical for molybdenyl ions with oxygen ligands (see Che *et al* 1979, Goldstein *et al* 1987, Serwicka 1984). Assuming that $\bar{E}_\parallel$ and $\bar{E}_\perp$ do not vary appreciably with glass composition, we get the mean bonding parameters summarized in table 3 and shown in figure 7 versus the content of phosphorus pentoxide. The magnitudes of variations in $\overline{\beta_1^2}$ and $\overline{\varepsilon^2}$, as can be seen from equations (12) and (13), would be somewhat altered if the assumption of constant energy level splittings was rejected. However, for any reasonable size of variations in $\bar{E}_\parallel$ and $\bar{E}_\perp$ with glass composition, the general tendencies would remain the same: $\overline{\beta_2^2}$ (and $\bar{\kappa}$) increase as $\overline{\beta_1^2}$ and $\overline{\varepsilon^2}$ decrease (see figure 7). At first sight, this seems rather unusual, since higher $\overline{\beta_2^2}$ (and $\bar{\kappa}$) values correspond to less covalent bonding, while lower $\overline{\beta_1^2}$ and $\overline{\varepsilon^2}$ indicate a higher degree of covalency. Such behaviour can be accounted for on the basis of the following

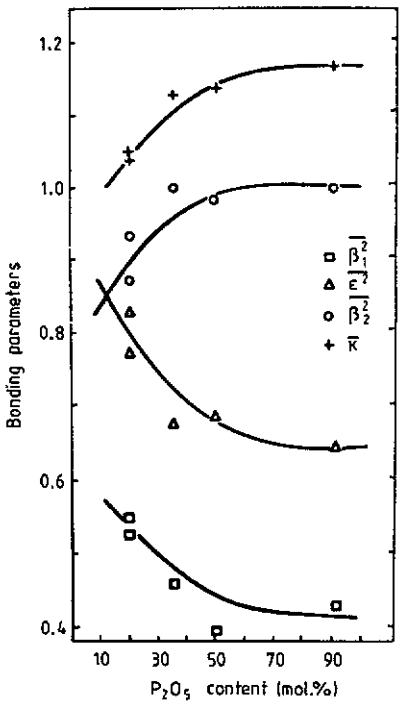

Figure 7. Mean bonding parameters as a function of phosphorus pentoxide content in WO_3–BaO–P_2O_5 glasses.

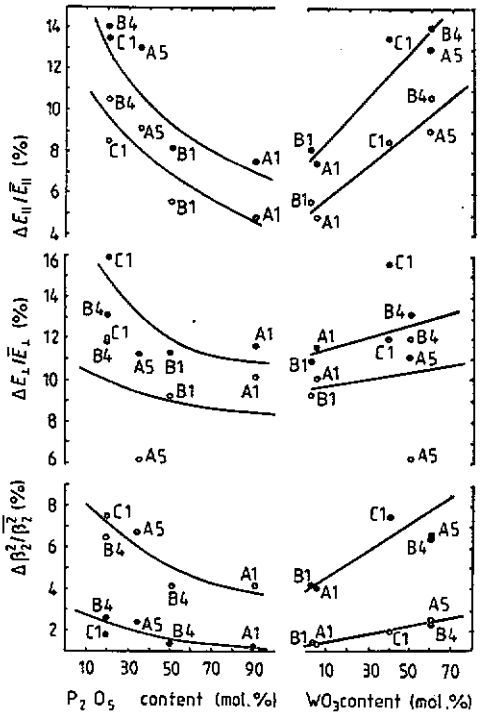

Figure 8. Relative distribution widths of energy level splittings and bonding parameters as functions of glass compositions. Open symbols refer to the case when all correlation coefficients between different parameters are set to zero. Full symbols correspond to the choice of correlation coefficients in accordance with (22). The lines drawn are guides to the eye.

reasoning. It is evident that phosphorus–oxygen bonds are more covalent in comparison with barium–oxygen or tungsten–oxygen bonds. Therefore, in the latter cases a higher *absolute* value of negative charge on the oxygen ligands is expected. Consequently, in glasses with lower phosphorus pentoxide content, where the probability of finding barium or tungsten in the second shell of Mo^{5+} is higher, stronger molybdenum–oxygen bonding and shorter mean Mo–O interatomic distances should occur. A similar conclusion has been reached by Studer *et al* (1986) in relation to W^{5+} ions in phosphate glasses.

Thus, two opposite trends can be, in principle, observed for the mean bonding parameters, as the glass composition is varied. On the one hand, for shorter Mo–O distances, the density of the unpaired electron of Mo^{5+} on the ligands should increase. On the other hand, owing to a concomitant increase of *negative* ligand charge, the density of the unpaired electron will be repelled from the ligands onto the central atom.

It is evident that the first trend should predominate for those Mo^{5+} orbitals which to a lesser extent overlap with the ligand orbitals, namely, for the ground B_2 state. Indeed,

one can see that the parameter $\overline{\beta_2^2}$, which describes the contribution of the d_{xy} Mo^{5+} orbital to the ground-state molecular orbital, increases in glasses with higher phosphorus pentoxide contents (hence, presumably, with shorter mean Mo–O distances). On the contrary, for Mo^{5+} orbitals overlapping to a greater extent with the ligands, the predominant effect should be the electrostatic repulsion. This is the case with the excited states E and, especially, B_1: the parameters $\overline{\varepsilon^2}$ and $\overline{\beta_1^2}$, which describe the contributions, respectively, of d_{xz} (d_{yz}) and $d_{x^2-y^2}$ Mo^{5+} orbitals to the corresponding molecular orbitals (see equations (11)), decrease as the phosphorus pentoxide content increases, in agreement with the presumed decrease of electrostatic repulsion.

4.3. Electron spin resonance and disorder of the glass structure

From equations (12) to (15) it is seen that the distributions of the g values and HFS parameters for Mo^{5+}, in principle, can be related to distributions of energy level splittings and bonding parameters.

In previous attempts to obtain numerical estimates of disorder parameters in glasses from ESR data, the distributions of either energy level splittings (Froncisz and Hyde 1980, Momo *et al* 1984) or bonding parameters (Bals and Kliava 1983, Kliava and Bals 1984) were neglected. Nicula and Culea (1987) estimated the distribution widths of both $g_\parallel$ and $A_\parallel$ for V^{4+} ion in oxide glasses using rather arbitrary assumptions concerning the distributions of energy level splittings *and* bonding parameters. Their estimates, however, have not been tested by computer simulations of the ESR spectra.

In the present study, we have attempted to evaluate the distribution widths of *both* energy level splittings and bonding parameters. The following general expression has been used:

$$\Delta H_k^2 = \sum_i \sum_j \left(\frac{\partial H_k}{\partial h_i} \frac{\partial H_k}{\partial h_j} \right)_{\substack{\Delta h_i \Delta h_j \rho(h_i, h_j) \\ h_i = \bar{h}_i, h_j = \bar{h}_j}} \tag{16}$$

where h_i and h_j are random parameters $E_\parallel$, $E_\perp$, β_1^2, β_2^2, ε^2 and κ, Δh_i and Δh_j are their RMS deviations, and $\rho(h_i, h_j)$ are correlation coefficients, $\rho(h_i, h_i) = 1$.

If all correlation coefficients for $i \neq j$ are equal to zero, equations (12) to (16) result in

$$(\Delta g_\parallel)^2 = (64\lambda^2/\bar{E}_\parallel^2)[(\overline{\beta_1^2}\,\overline{\beta_2^2}\Delta E_\parallel/\bar{E}_\parallel)^2 + (\overline{\beta_1^2}\Delta\beta_2^2)^2 + (\overline{\beta_2^2}\Delta\beta_1^2)^2] \tag{17}$$

$$(\Delta g_\perp)^2 = (4\lambda^2/\bar{E}_\perp^2)[(\overline{\beta_2^2}\,\overline{\varepsilon^2}\Delta E_\perp/\bar{E}_\perp)^2 + (\overline{\beta_2^2}\Delta\varepsilon^2)^2 + (\overline{\varepsilon^2}\Delta\beta_2^2)^2] \tag{18}$$

$$(\Delta A_\parallel/P)^2 = (\kappa + \tfrac{4}{7})^2(\Delta\beta_2^2)^2 + (\overline{\beta_2^2}\Delta\kappa)^2 + (\Delta g_\parallel)^2 + \tfrac{9}{49}(\Delta g_\perp)^2 \tag{19}$$

$$(\Delta A_\perp/P)^2 = (\kappa - \tfrac{2}{7})^2(\Delta\beta_2^2)^2 + (\overline{\beta_2^2}\Delta\kappa)^2 + \tfrac{121}{196}(\Delta g_\perp)^2. \tag{20}$$

Making natural, though somewhat arbitrary, assumptions that

$$(\Delta\beta_1^2/\overline{\beta_1^2}) = (\Delta\beta_2^2/\overline{\beta_2^2}) = (\Delta\varepsilon^2/\overline{\varepsilon^2}) \tag{21}$$

one can solve the resulting system of equations for $\Delta E_\parallel$, $\Delta E_\perp$, $\Delta\beta_2^2$ and $\Delta\kappa$. The results of these calculations are listed in table 3.

In order to estimate the influence exerted on these parameters by non-zero correlations between different random variables, the following set of $\rho(h_i, h_j)$ can be considered:

	h_j					
h_i	$E_\parallel$	$E_\perp$	β_2^2	ε^2	β_1^2	κ
$E_\parallel$	1	1	−1	1	1	−1
$E_\perp$	1	1	−1	1	1	−1
β_2^2	−1	−1	1	−1	−1	1
ε^2	1	1	−1	1	1	−1
β_1^2	1	1	−1	1	1	−1
κ	−1	−1	1	−1	−1	1

(22)

Such a choice of *signs* of the correlation coefficients is consistent with the reasoning presented and the tendencies described in the previous section, as well as taking into account the obvious fact that the energy level splittings increase as the negative ligand charge is increased and/or the Mo–O distance is shortened.

In this case, one obtains from equations (12) to (16) and (22):

$$\Delta g_\parallel = 8\lambda\overline{\beta_1^2}\,\overline{\beta_2^2}\,\Delta E_\parallel/\bar{E}_\parallel^2 \tag{23}$$

$$\Delta g_\perp = 2\lambda\overline{\beta_2^2}\,\overline{\varepsilon^2}\,\Delta E_\perp/\bar{E}_\perp^2 \tag{24}$$

$$\Delta A_\parallel/|P| = (\bar{\kappa} + \tfrac{4}{7})\Delta\beta_2^2 + \overline{\beta_2^2}\Delta\kappa + \Delta g_\parallel + \tfrac{3}{7}\Delta g_\perp \tag{25}$$

$$\Delta A_\perp/|P| = (\bar{\kappa} - \tfrac{2}{7})\Delta\beta_2^2 + \overline{\beta_2^2}\Delta\kappa + \tfrac{11}{14}\Delta g_\perp. \tag{26}$$

The results of solving the system of equations (23) to (26) are also listed in table 3.

It should be understood that, in reality, $\rho(h_i, h_j)$ for $i \neq j$ hardly equal zero; however, they never approach unity in absolute value. Thus, the actual values of distribution widths of the energy level splittings and bonding parameters are believed to lie between those corresponding to the limiting cases considered above.

Figure 8 displays the dependence of $\Delta E_\parallel/\bar{E}_\parallel$, $\Delta E_\perp/\bar{E}_\perp$ and $\Delta\beta_2^2/\overline{\beta_2^2}$ on glass composition. One can see that both $\Delta E_\parallel$ and $\Delta\beta_2^2$ and, less distinctly, $\Delta E_\perp$ tend to increase as (i) the content of tungsten trioxide is increased and (ii) the content of phosphorus pentoxide is decreased. Note that, in spite of the pronounced dependence of the magnitudes of these parameters on the choice of correlation coefficients, these tendencies are well preserved. It can be concluded that in multicomponent glasses the degree of short-range disorder to a considerable extent depends on the glass composition.

As is apparent from table 3, the estimates of distribution widths of energy level splittings for various glass compositions are confined within the following limits: $5\% < \Delta E_\parallel/\bar{E}_\parallel < 14\%$; $7\% < \Delta E_\perp/\bar{E}_\perp < 16\%$. Those of bonding parameters do not exceed a few per cent: $1.3\% < \Delta\beta_2^2/\overline{\beta_2^2} < 7.5\%$. These findings, together with the previous ones, namely that relative distribution widths of the Mo–O (and W–O) bond lengths in phosphate glasses are about 2–3% (Bals and Kliava 1983, Kliava and Bals 1984), give support to the viewpoint according to which the short-range order in glasses is relatively well preserved.

Last, it should be pointed out that both the characteristics of 'average' sites and the short-range disorder parameters for Mo^{5+} ions contain some indications on the presumed dichotomy between the structural role of tungsten above and below the orthophosphate line. On the other hand, one might argue that there are only certain gradual variations

in the structure of the environment of Mo^{5+} ions and in the amount of short-range disorder as the glass composition is varied.

Nevertheless, it is interesting to note that, as one can see from figure 8, Mo^{5+} ions possess a more ordered environment in glasses with high P_2O_5 content and/or low WO_3 content, in which molybdenum is supposed to substitute for tungsten at network modifier sites. At the same time, in the region above the orthophosphate line, where molybdenum presumably substitutes for tungsten at network former sites, a higher degree of short-range disorder occurs. We remind the reader that an analogous conclusion has been reached earlier in relation to two different Mn^{2+} sites, with $g = 2.0$ and $g = 4.3$, in oxide glasses (Kliava 1982, 1986).

5. Concluding remarks

The main problem that one has to deal with in ESR studies of disordered solids is the high number of parameters to be deduced from computer simulations of the ESR spectra. This may result in an ambiguity in the best-fit parameters obtained.

For some paramagnetic ions, such as Mo^{5+}, isotopic enrichment permits one, using a gradual parametrization procedure, to determine separately the g values as well as the HFS parameters. This substantially extends the accuracy and reliability of information deduced from experimental ESR spectra.

Using a computer simulation approach that explicitly takes into account distributions of the spin Hamiltonian parameters, the characteristics can be determined of both the 'average' paramagnetic sites (degree of distortion from cubic symmetry, mean energy level splittings and mean bonding parameters) and of short-range disorder (root-mean-square deviations of energy level splittings and bonding parameters). In the present study, it has been demonstrated that in molybdenum-doped WO_3–BaO–P_2O_5 glasses of various compositions the degree of rhombic distortion of the 'average' Mo^{5+} site is related to the difference in size of atoms forming the second coordination shell of molybdenum, while the degree of axial distortion depends on tungsten trioxide content. As the glass composition is varied, the mean values of bonding parameters show consistent trends, which can be accounted for by concomitant variations in the Mo–O bond lengths and in the ligand charges.

Using more or less judicious simplifying assumptions, we have been able to estimate separately the RMS deviations of energy level splittings and bonding parameters for Mo^{5+}. It is shown that a rather moderate amount of short-range disorder occurs in WO_3–BaO–P_2O_5 glasses. Concerning the presumably ambivalent structural role of tungsten in these glasses (that of network former or network modifier), the widely acknowledged concept of well ordered network former sites and ill defined network modifier sites is not confirmed. Evidence is given rather in support of the opposite viewpoint.

In summary, the present study highlights the significance of next nearest neighbours in determining the structure of a site in glass. Indeed, from the viewpoint of short-range ordering the main consequence of varying the composition of ternary phosphate glass is a replacement of different atoms (P, W or Ba) in the second coordination shell of an atom in question (molybdenum). It is demonstrated that this replacement perceptibly modifies such structural features as the degree of axial and rhombic distortion in the environment of molybdenum ions, the covalency of metal–ligand bonds and the amount of short-range disorder, which manifests itself in distributions of energy level splittings

and bonding parameters. The last item implies that the short-range disorder in multicomponent glasses is closely related to the compositional or chemical disorder.

References

Bals A and Kliava J 1983 *J. Magn. Reson.* **53** 243–58

Bals A, Kliava J and Purâns J 1980 *J. Phys. C: Solid State Phys.* **13** L437–41

Bielis I J and Millere I V 1975 *Physics and Chemistry of Glass-Forming Systems* (Fizika i himija steklo-obrazujushchih sistem) vol 3 (Rīgā: University of Latvia) pp 136–50

—— 1977 *Physics and Chemistry of Glass-Forming Systems* (Fiziki i himija stekloobrazujushchih sistem) vol 5 (Rīgā: University of Latvia) pp 50–60

Che M, Fournier M and Launay J P 1979 *J. Chem. Phys.* **71** 1954–60

Daul C, Schläpfer C W, Mohos B, Ammeter J and Gamp E 1981 *Comput. Phys. Commun.* **21** 385–95

de Armond K, Garrett B B and Gutovsky H S 1965 *J. Chem. Phys.* **42** 1019–25

Froncisz W and Hyde J S 1980 *J. Chem. Phys.* **73** 3123–31

Golding R M and Tennant W C 1973 *Mol. Phys.* **25** 1163–71

Goldstein A, Chiriac V and Becherescu D 1987 *J. Non-Cryst. Solids* **92** 271–7

Greaves G N 1985 *J. Non-Cryst. Solids* **71** 203–17

Griscom D L 1980 *J. Non-Cryst. Solids* **40** 211–72

Hecht H G and Johnston T S 1967 *J. Chem. Phys.* **46** 23–34

Kliava J 1982 *J. Phys. C: Solid State Phys.* **15** 7017–29

—— 1986 *Phys. Status Solidi* b **134** 411–55

—— 1988 *ESR Spectroscopy of Disordered Solids* (EPR spectroskopija neuporiadochennyh tverdyh tel) (Rīgā: Zinātne)

Kliava J and Bals A 1984 *Fiz. Him. Stekla* (Leningrad) **10** 47–52

Latef A, Elamrani R, Gengembre L, Aissi C F, Kasztelan S, Barbaux Y and Guelton M 1987 *Z. Phys. Chem.* **152** 93–103

Louis C and Che M 1987 *J. Phys. Chem.* **91** 2875–83

Momo F, Sotgiu A, Bettinelli M and Montenero A 1984 *Phys. Status Solidi* a **81** K27–30

Nicula A and Culea E 1987 *Phys. Status Solidi* b **142** 265–70

Peterson G E, Kurkjian C R and Carnevale A 1974 *Phys. Chem. Glasses* **15** 52–8

Pilbrow J R and Lowrey M R 1980 *Rep. Prog. Phys.* **43** 433–95

Rawson H 1967 *Inorganic Glass-Forming Systems* (New York: Academic)

Selvaraj U and Rao K J 1988 *Chem. Phys.* **123** 141–50

Serwicka E 1984 *J. Solid State Chem.* **51** 300–6

Shannon R D and Prewitt C T 1969 *Act Crystallogr.* B **25** 925–46

Studer F, Lebail A and Raveau B 1986 *J. Solid State Chem.* **63** 414–23

Studer F, Rih N and Raveau B 1988 *J. Non-Cryst. Solids* **107** 101–17

Taylor P C, Baugher J F and Kriz H M 1975 *Chem. Rev.* **75** 203–40

Zachariasen W H 1932 *J. Am. Chem. Soc.* **54** 3841–51